



Recent MHD topics in Large Helical Device

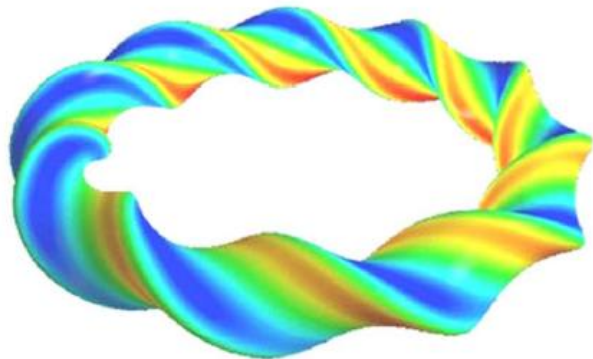
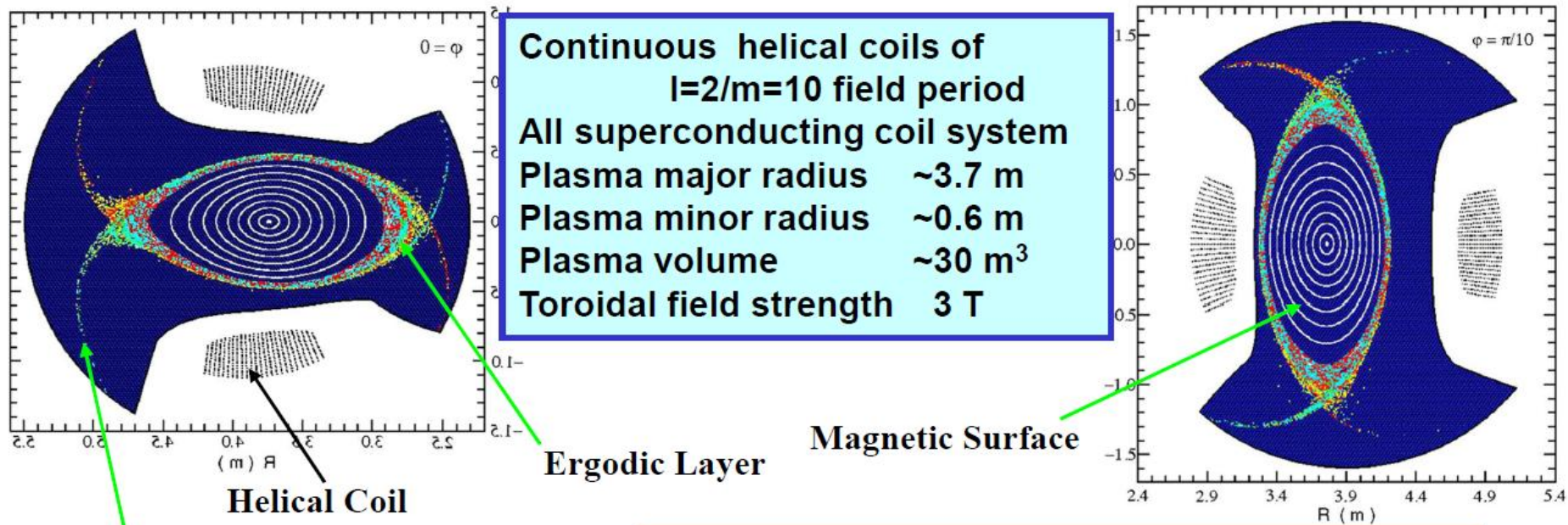
Yuki Takemura

National Institute for Fusion Science

25th Coordinated Working Group Meeting of the Stellarator-
Heliotron Technology Collaboration Programme(CWGM)

June 3-5th, 2025 in PPPL

Structure and plasma achievement of LHD



High beta

$$\langle \beta \rangle = 5.1 \% \text{ at } B = 0.43 \text{ T}$$

$$\langle \beta \rangle = 4.1 \% \text{ at } B = 1.0 \text{ T}$$

High density

$$n_e(0) = 1.2 \times 10^{21} \text{ m}^{-3} \text{ at } B = 2.5 \text{ T}$$

High ion temperature

$$T_i = 10 \text{ keV at } n_e = 1.6 \times 10^{19} \text{ m}^{-3}$$

High ion and electron temperature

$$T_i \text{ 8.7 keV} / T_e \text{ 8.7 keV at } n_e = 1.6 \times 10^{19} \text{ m}^{-3}$$

Long pulse : 1.2MW for 48min.

$$\text{Fusion product; } n \tau_E T = 5 \times 10^{19} \text{ m}^{-3} \text{ s keV}$$

Outline

This presentation highlights recent research outcomes on MHD phenomena in the LHD experiment, with the aim of fostering collaborative studies across the helical device community

- The final LHD experiment campaign will be held from mid-September to the end of December 2025.

We introduce four key topics that address challenges commonly shared among helical systems:

- External RMP physics
- Magnetic Island Dynamics
- Frequency determination mechanisms of MHD activities
- AI-Assisted Prediction of Abrupt MHD Events

External RMP physics

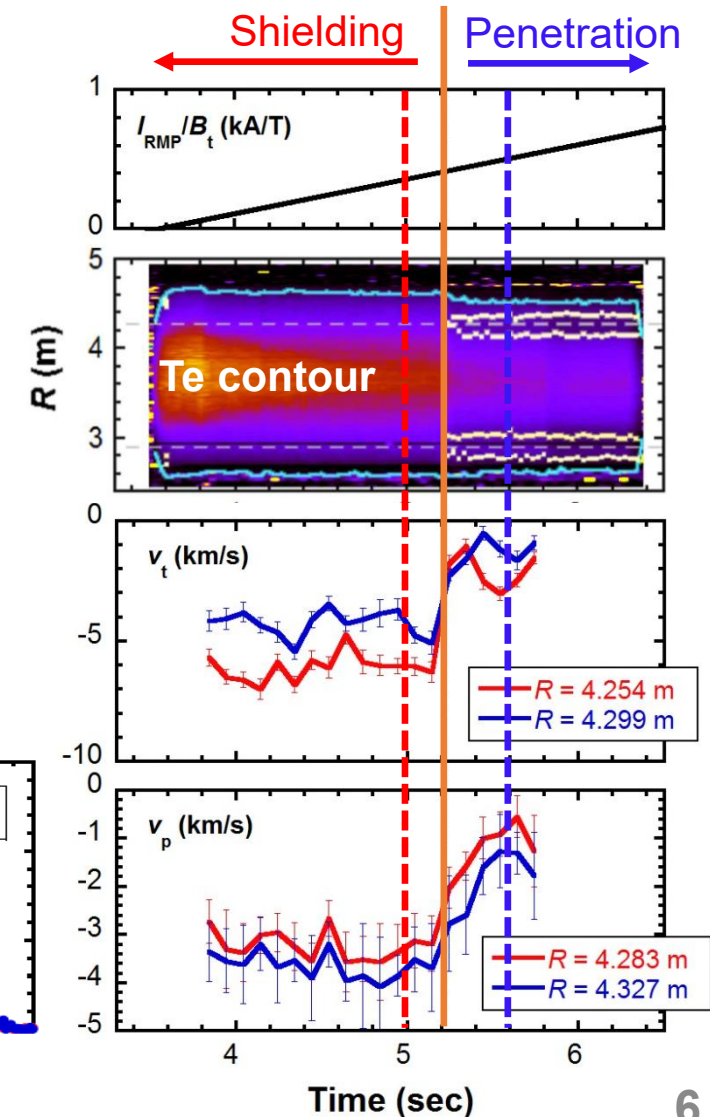
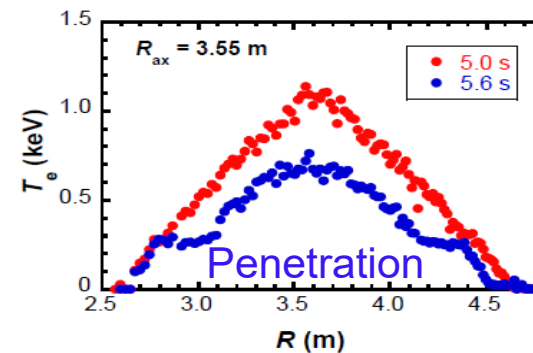
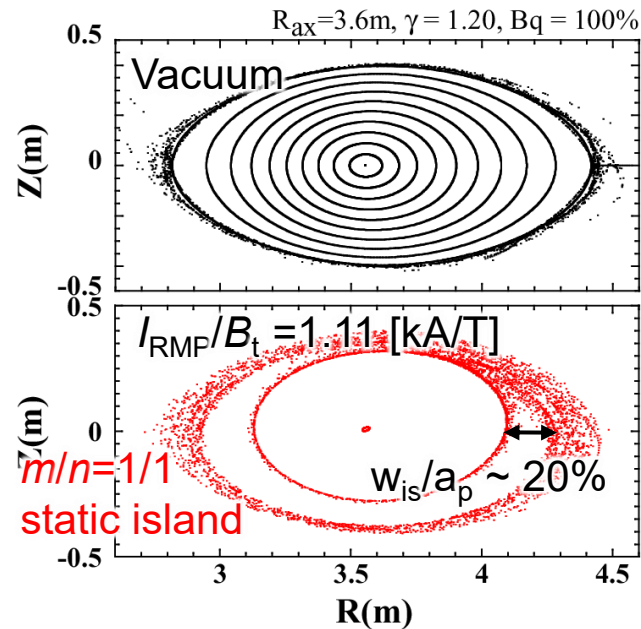
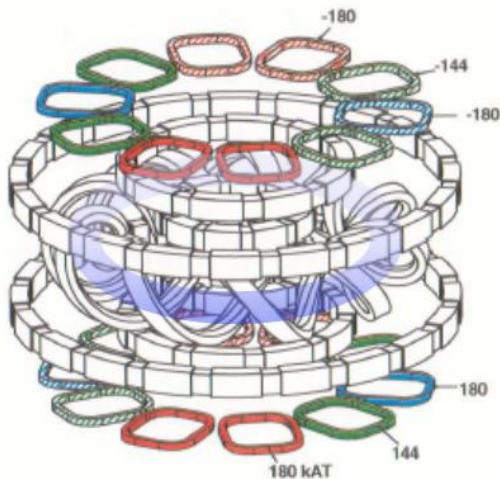
- RMP Stabilization of MHD Instabilities
- Modelling of RMP penetration thresholds

Topics of external RMP

- In tokamaks, external RMPs have been successfully applied to stabilize RWMs and ELMs [Evans et al., Nature Physics **2**, 419–423 (2006)]
- In helical plasmas, the stabilization of **resistive interchange modes**, which are pressure-driven instabilities, has also been experimentally demonstrated using external RMPs [Ito et al., PFR 18, 2402007 (2023)]
 - **Understanding the scaling of stabilization conditions is essential for extrapolating to future fusion devices.**
- However, when the applied RMP is too strong, it may **penetrate into the plasma**, leading to the formation of large magnetic islands and subsequent degradation of confinement.
 - **To prevent undesirable effects, it is essential to develop a predictive model that captures the physics of RMP penetration.**

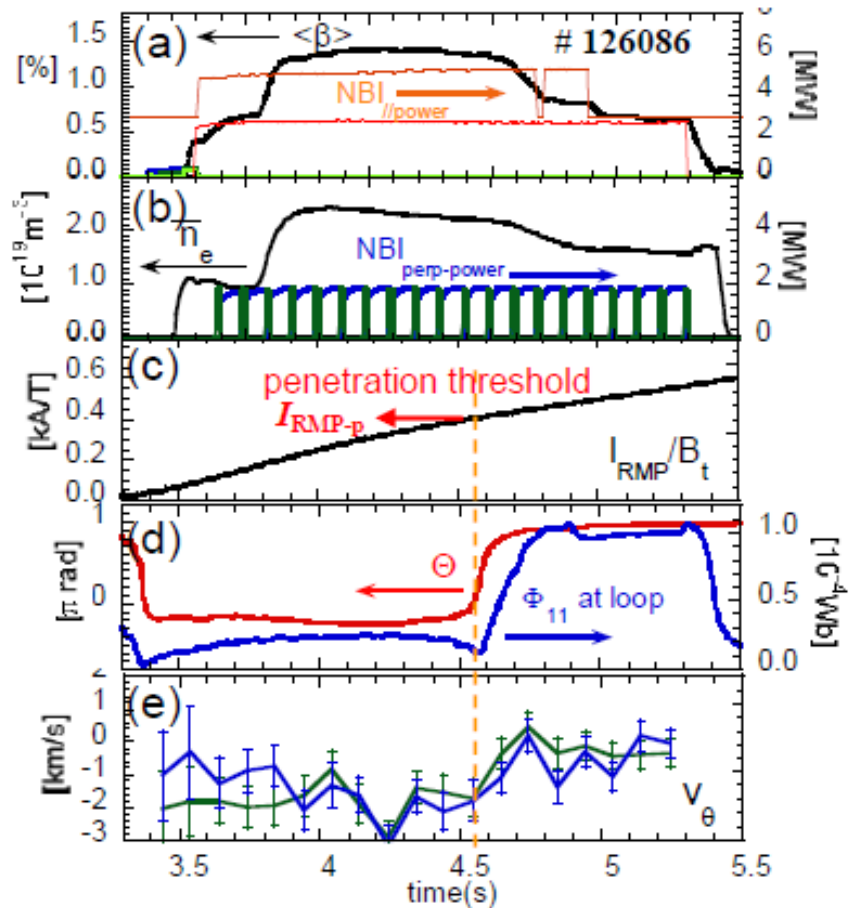
RMP coil system and example of RMP penetration

- RMP coil system can alter spatial structure (mainly $m/n = 1/1$, or $2/1$), width and position of formed magnetic islands
 - If external RMP penetrates to plasmas and forms magnetic islands, confinement property is significantly reduced
- Important to control MHD instabilities keeping its shielding



Dependence of RMP penetration threshold on plasma parameters in LHD

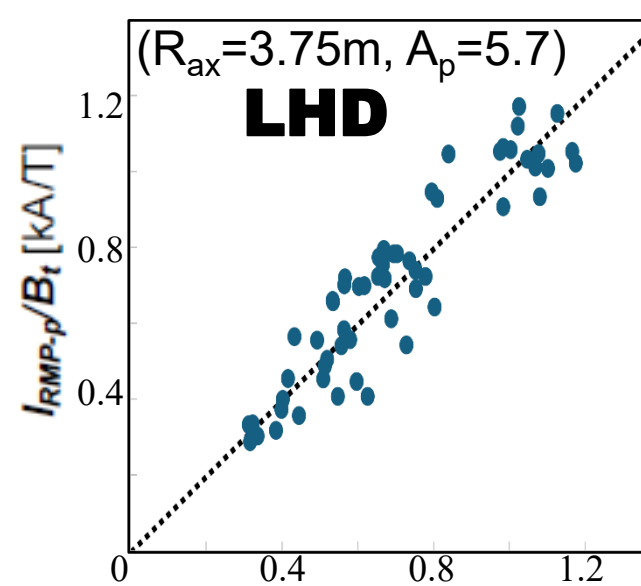
Rump-up RMP experiment



RMP penetration threshold scaling in Ohmic tokamak discharges

[Y. GIRBOV, in Meeting of ITPA MHD TG, Oct. 2017]

$$B_{\text{pen}} / B_t \propto n_e^{1.4 \pm 0.13} B_t^{-1.8 \pm 0.16} R^{0.81 \pm 0.24} \beta_N^{-0.86 \pm 0.14}$$



Threshold dependence on n_e and B_t is qualitative similar with that in Ohmic tokamak plasmas, and the dependence on β is opposite to the tokamaks.

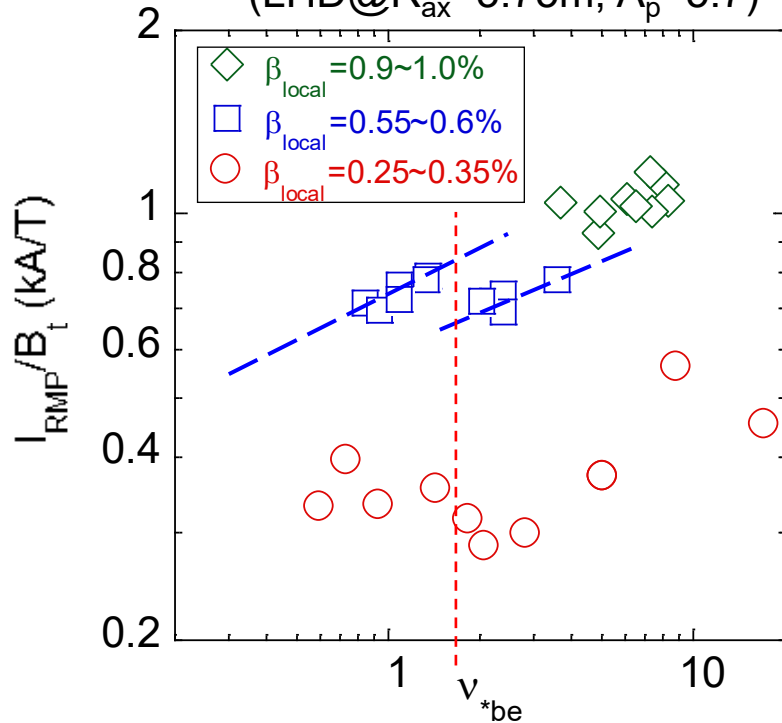
$$0.78 \cdot \beta^{1.2} \cdot v_{*b}^{-0.038} \cdot \rho_*^{-0.48} \propto n_e^{0.35} \cdot B_t^{-0.15} \cdot \beta^{0.88}$$

- Shielding mechanism is different between helical and tokamak!!
- Why does this scattering occur? → **How about the collisionality effect?**

Dependence of RMP penetration threshold on plasma parameters in LHD (II)

Dependence on collisionality

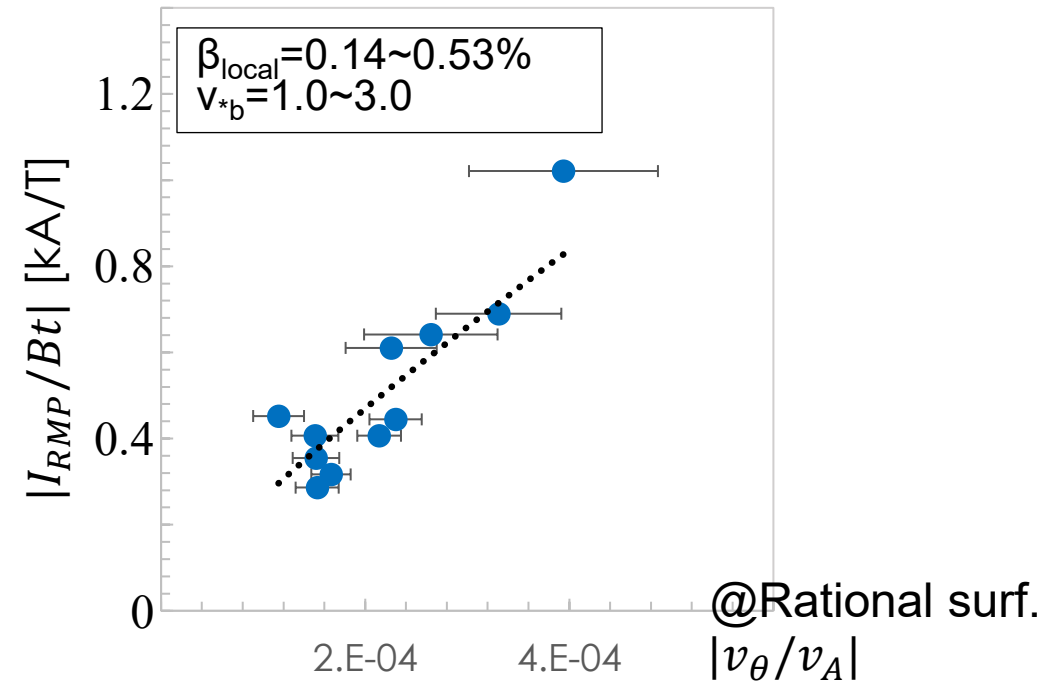
(LHD@ $R_{ax}=3.75\text{m}$, $A_p=5.7$)



Dependence seems to change depending on the collisionality regimes.

Dependence on poloidal velocity

(LHD@ $R_{ax}=3.75\text{m}$, $A_p=5.7$)



Pen. threshold is proportional to the normalized poloidal flow velocity with high correlation.

→ The determination mechanism is likely related to **poloidal NC viscosity**, which governs poloidal flow and varies with the collisionality regime in helical plasmas.

Dependence of RMP penetration threshold on plasma parameters in LHD (III)

Model Eqs. [Nishimura PoP 2012]

Time evolution of island width (w)

$$\frac{dw}{dt} = -\frac{\eta_{||}\Delta'_0}{I_1\mu_0} \left(\frac{aI_{RMP}/B}{w^2} \cos \Theta - 1 \right)$$

Time evolution of island phase (Θ)

$$\frac{\partial \Theta}{\partial t} = -\frac{v_\theta}{r_s}$$

Momentum eq. of poloidal flow velocity (v_θ)

$$\frac{\partial v_\theta}{\partial t} = -C \Delta'_0 \frac{I_{RMP}}{B} w \sin \Theta - \frac{e}{\varepsilon_\perp B} (\Gamma_i^{neo} - \Gamma_e^{neo})$$

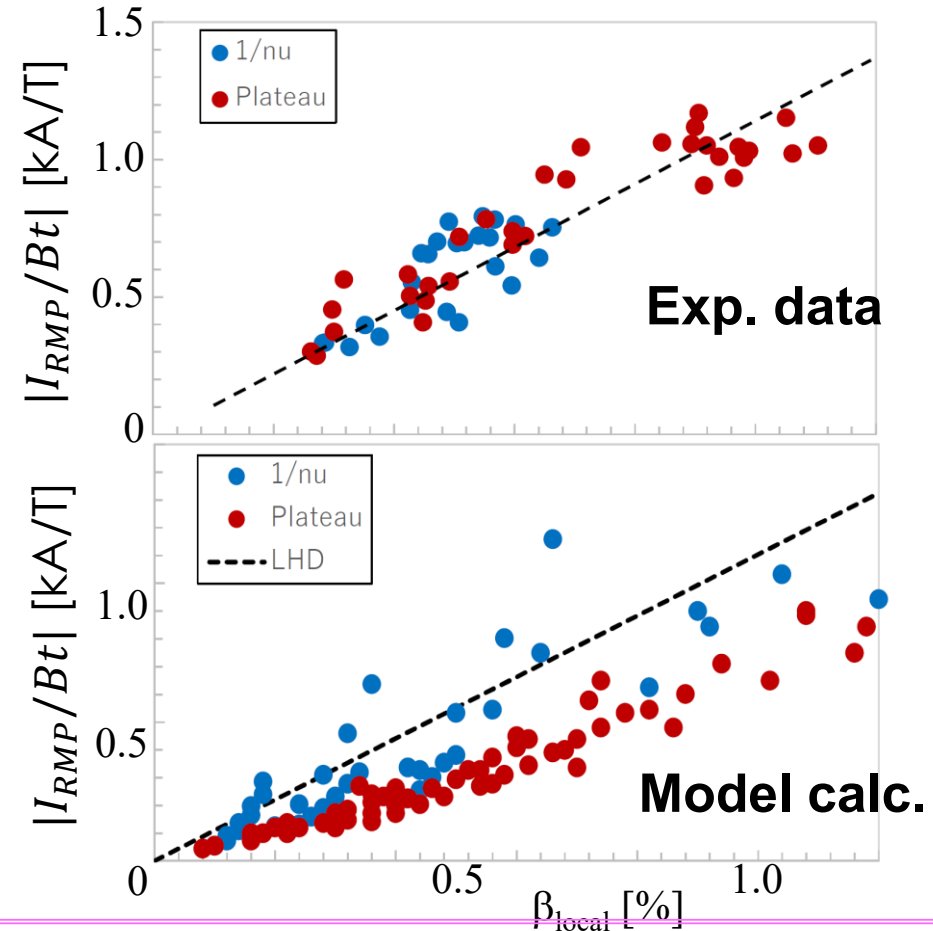
$$\Gamma_a^{neo} (NC \text{ radial particle flux}) \propto \langle \mathbf{B}_\theta \cdot \nabla \cdot \mathbf{\Pi}_a \rangle (pol. \text{ viscos})$$

1/ ν -regime

$$-\frac{e}{\varepsilon_\perp B} \Gamma_i^{\frac{1}{\nu}} = \frac{\varepsilon_t^2 \varepsilon_h^{1.5} v_A^2}{12 r_s^2} \frac{1}{v_{tha}} \beta \left(\frac{T_i}{q_i B} \left(\frac{n'_i}{n_i} + \frac{T'_i}{T_i} - \frac{q_i B}{T_i} v_\theta \right) \right)$$

plateau regime

$$-\frac{e}{\varepsilon_\perp B} \Gamma_i^{pl} = \frac{5\sqrt{\pi}(1+5\varepsilon_t^2)\varepsilon_t\varepsilon_h^2v_A^2}{8r_s(T_i/m_i)^{0.5}} \beta \left(\frac{T_i}{q_i B} \left(\frac{n'_i}{n_i} + \frac{3T'_i}{2T_i} - \frac{q_i B}{T_i} v_\theta \right) \right)$$

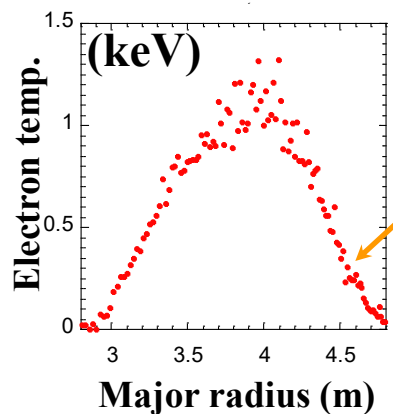
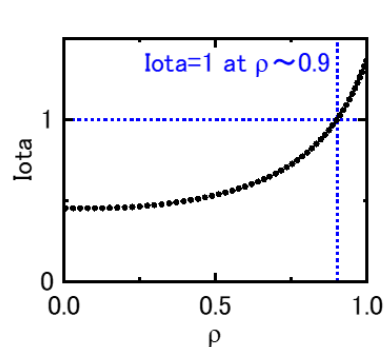
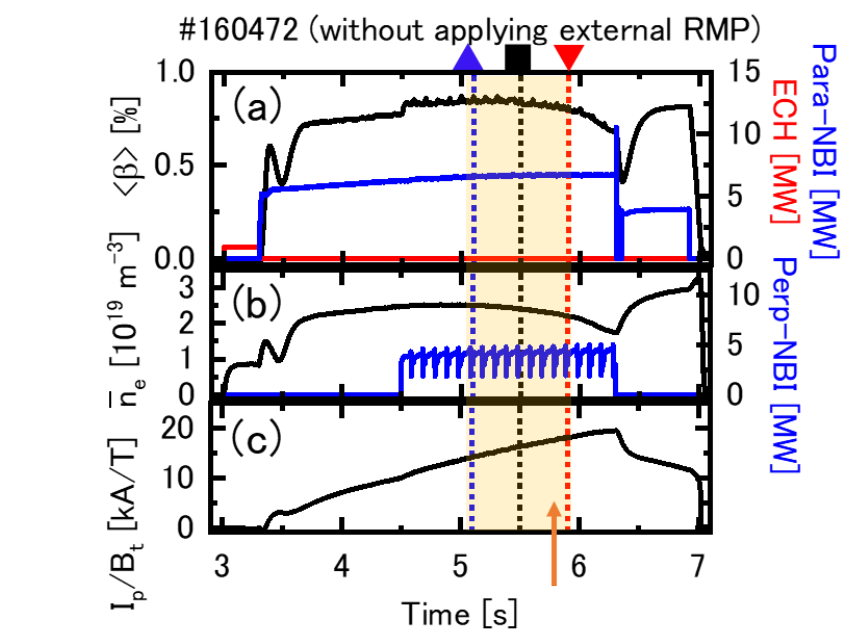


**Pred. of Model qualitatively coincides Exp. data.
However, quantitatively does not coincide.**

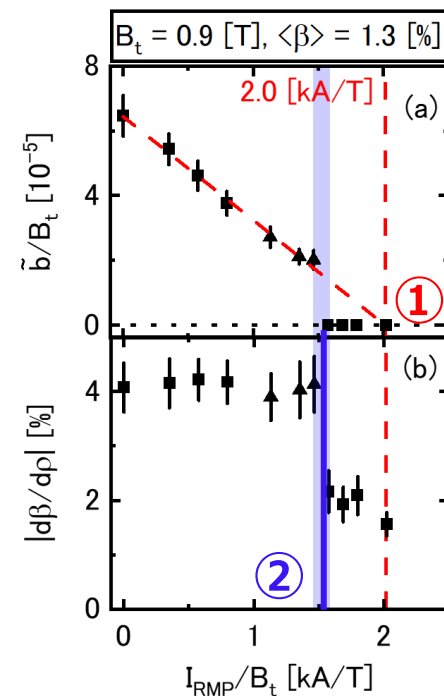
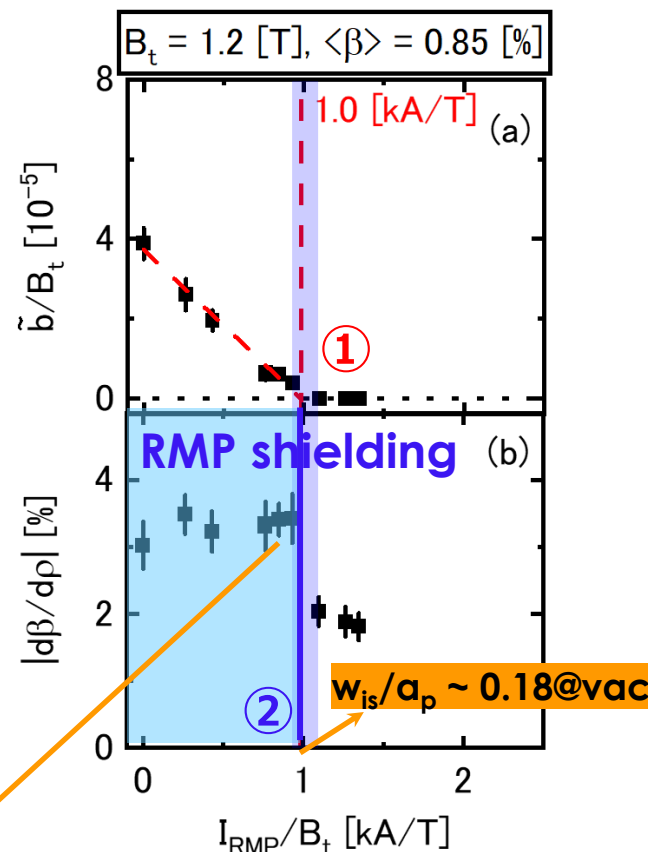
→ We should bluish up the model of NCV, or apply the other model like viscosity driven by turbulence???

Mode stabilization by RMP

Res.-Interchange insta. (RIC) response to ext.-RMP



Config. with mag. axis torus
location $R_{ax}=3.75m$



$m/n=1/1$ static external
RMP suppresses $m/n=1/1$
interchange instability with
the shielding of the Ext.-
RMP (with no degradation
of pressure gradient)

Amplitude of Ext.-RMP
depend on exp. conditions

- ① Ext.-RMP to completely
suppress Mag. fluc. (RIC-
mode stabilize)
- ② Penetration threshold of
ext.-RMP (Mag. island appears)

How do they depend??

Experiments to construct scaling laws

- In a same vacuum mag. configuration of the LHD, res. interchange insta. suppression experiments by ext.-RMP are done under the 20 series with various conditions of mag. field strength, electron density and heating power, which changes independently.

Operation regimes	
Mag. field strength@Mag. axis B_t [T]	0.75~1.7
Elec. density@res. surf. n_e [10^{19}m^{-3}]	1.7~4.6
Elec. temp.@res. surf. T_e [eV]	160~400

- Try to construct Scaling laws depending on 2 non-dimensional parameters for the following values with Multiple Regression Analysis

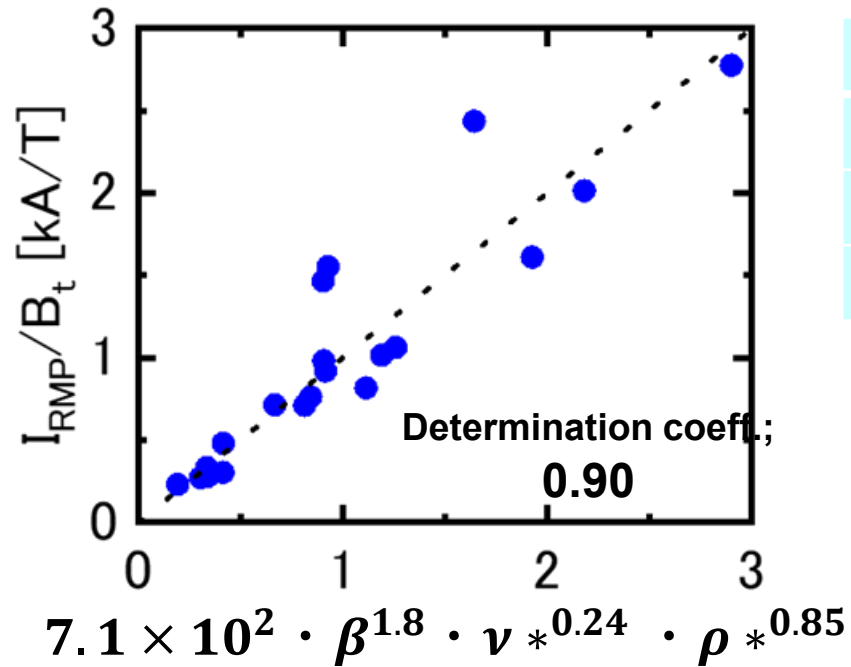
① **Amp. of ext.-RMP to completely suppress Mag. fluc.,**

② **Penetration threshold of ext.-RMP,**

As 3 independent non-dimensional parameters, we select the followings, which are commonly used for the confinement performance

Beta value; β , Normalized colisionality; ν^* , Normalized ion gyro-radius; ρ^*

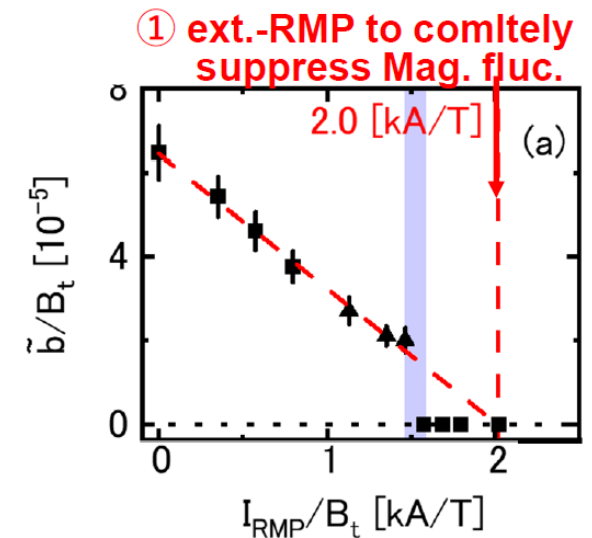
Scaling law for Ext.-RMP to completely suppress Mag. fluc.



Operation regimes	
Beta value; β	0.20~0.59
Normalized colisionality; ν^*	1.2~8.0
Normalized ion gyro-radius; ρ^*	0.0018~0.0033

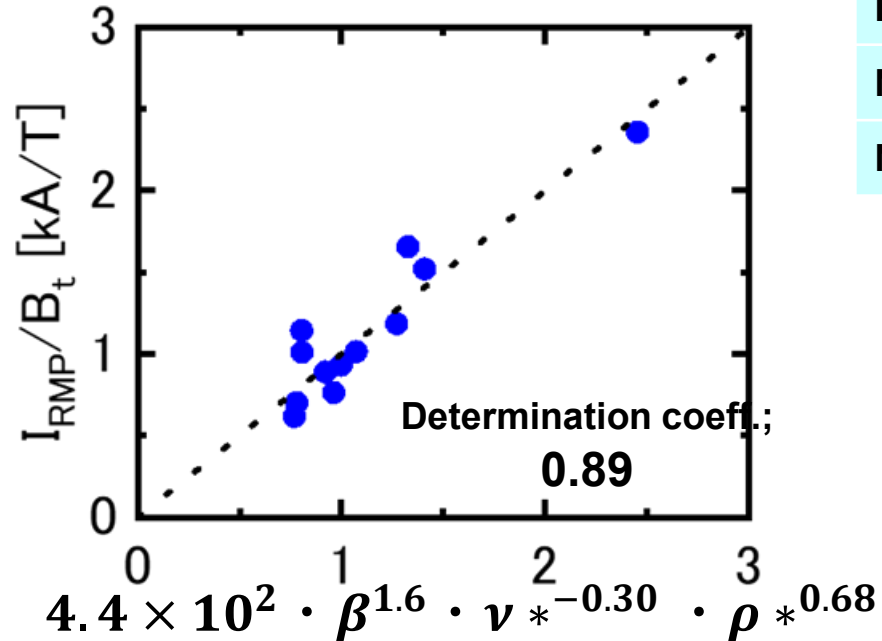
Correlation coeff.(Log)	
$\beta \Leftrightarrow \nu^*$	0.86
$\beta \Leftrightarrow \rho^*$	0.47
$\nu^* \Leftrightarrow \rho^*$	0.24

- **[Ext.-RMP amp. to completely suppress Mag. fluc.]**
 $= 7.1 \times 10^2 \cdot \beta^{1.8} \cdot \nu^{*0.24} \cdot \rho^{*0.85}$
- Note; Identification accuracy of the power of β and ν^* is relatively poor because correlation coeff. between β and ν^* .



Scaling law for penetration threshold of ext.-RMP

- Penetration of ext.-RMP is observed in 12 series among 20 experiment series



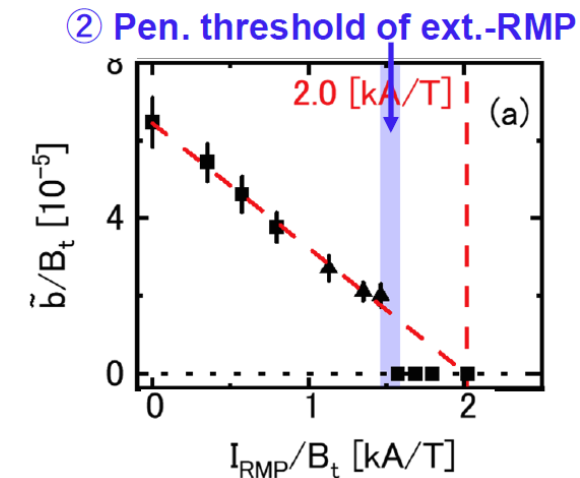
Operation regimes

Beta value; β	0.37~0.59
Normalized colisionality; ν^*	2.9~8.0
Normalized ion gyro-radius; ρ^*	0.0019~0.0033

Correlation coeff.(Log)

$\beta \Leftrightarrow \nu^*$	0.54
$\beta \Leftrightarrow \rho^*$	0.60
$\nu^* \Leftrightarrow \rho^*$	-0.06

- **[Pen. threshold of Ext.-RMP]**
 $= 4.4 \times 10^2 \cdot \beta^{1.6} \cdot \nu_*^{-0.30} \cdot \rho_*^{0.68}$



Summary for the scaling law

- Empirical scaling laws of ① Ext.-RMP to completely suppress Mag. fluc. and ② Penetration threshold of ext.-RMP on 3 non-dimensional parameters (β , ν^* , ρ^*) are obtained by Multiple Regression Analysis

$$\textcircled{1} [\text{Ext.-RMP to completely suppress Mag. fluc.}] = 7.1 \times 10^2 \cdot \beta^{1.8} \cdot \nu^{*0.24} \cdot \rho^{*0.85}$$

$$\textcircled{2} [\text{Penetration threshold of ext.-RMP}] = 4.4 \times 10^2 \cdot \beta^{1.6} \cdot \nu^{*-0.30} \cdot \rho^{*0.68}$$

- β and ρ^* dependence of ① and ② are similar. However, ν^* dependence of ① and ② is quite different, which leads to the following prediction;
- Operation regime to suppress instability without degradation due to ext.-RMP penetration is wider as the collisionality is lower under the same beta and normalized ion gyro-radius.

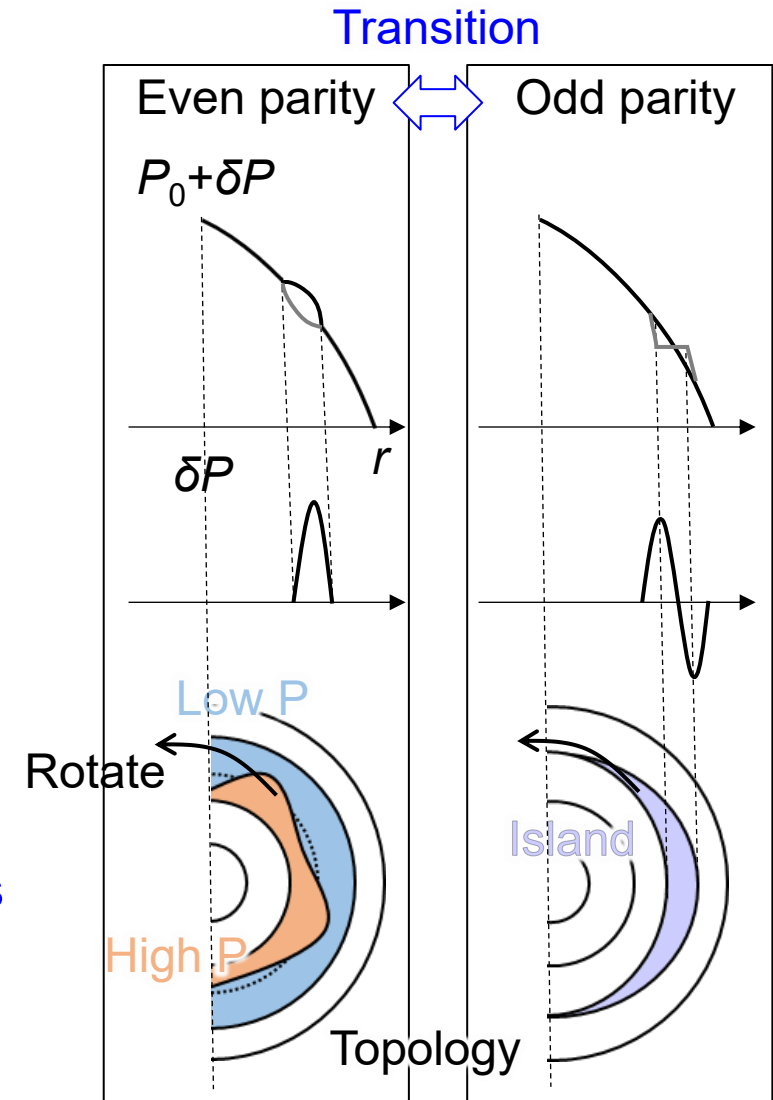
CAUTION!!!;

The situation would change because the pen. threshold dependence on collisionality changes depending on the mag. configuration. Ex. In $R_{ax}=3.60\text{m}$ config. , pen. threshold is proportional to $\nu^{*+??}$

Magnetic Island Dynamics

What is parity transition?

- In magnetically confined fusion plasmas, **parity of radial structure of MHD fluctuations** is strongly related to topology of magnetic vessel
 - Odd parity shows existence of island structure that degrades plasma confinement property
 - 'Parity transition' means rapid change in radial structure of dominant MHD fluctuation **while its toroidal/poloidal mode number(m/n) and mode location are maintained**
 - Parity transition corresponds to change in magnetic topology
 - Even-to-Odd transition: island formation
 - Odd-to-Even transition: island disappearance
- **Understanding physical mechanism of parity transition provides new insights into magnetic island physics**



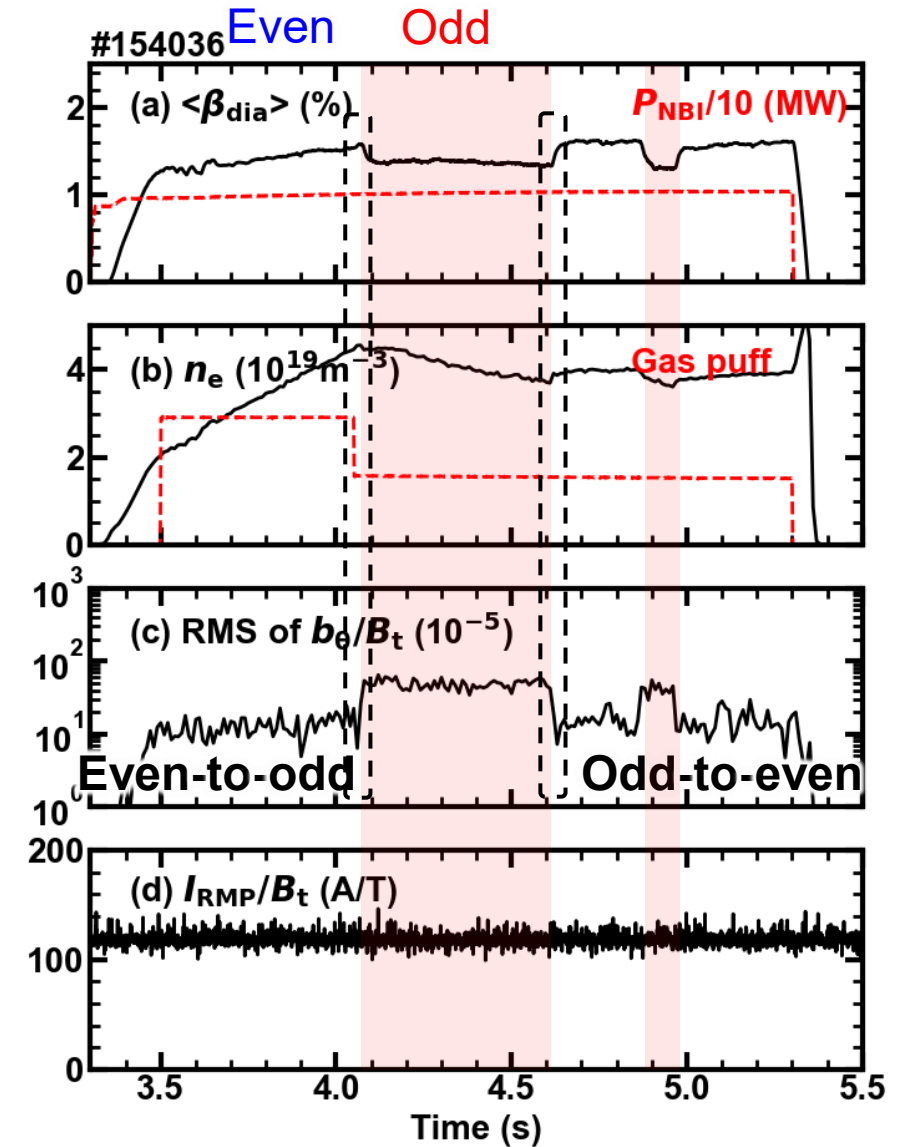
MHD Instabilities with Magnetic Islands in LHD and Island Formation/Disappearance

- The most expected MHD instability in LHD is the **resistive interchange mode**.
 - According to linear theory, RIC is **not accompanied by magnetic island formation**.
 - Indeed, observed MHD fluctuations have the local mode structure with no island [Watanabe et al., Phys. Plasmas, 2011].
- However, under specific experimental conditions, **an instability with an island has been observed** [Takemura et al., Phys. Plasmas, 2022].

In addition, **parity transitions** have been reported:

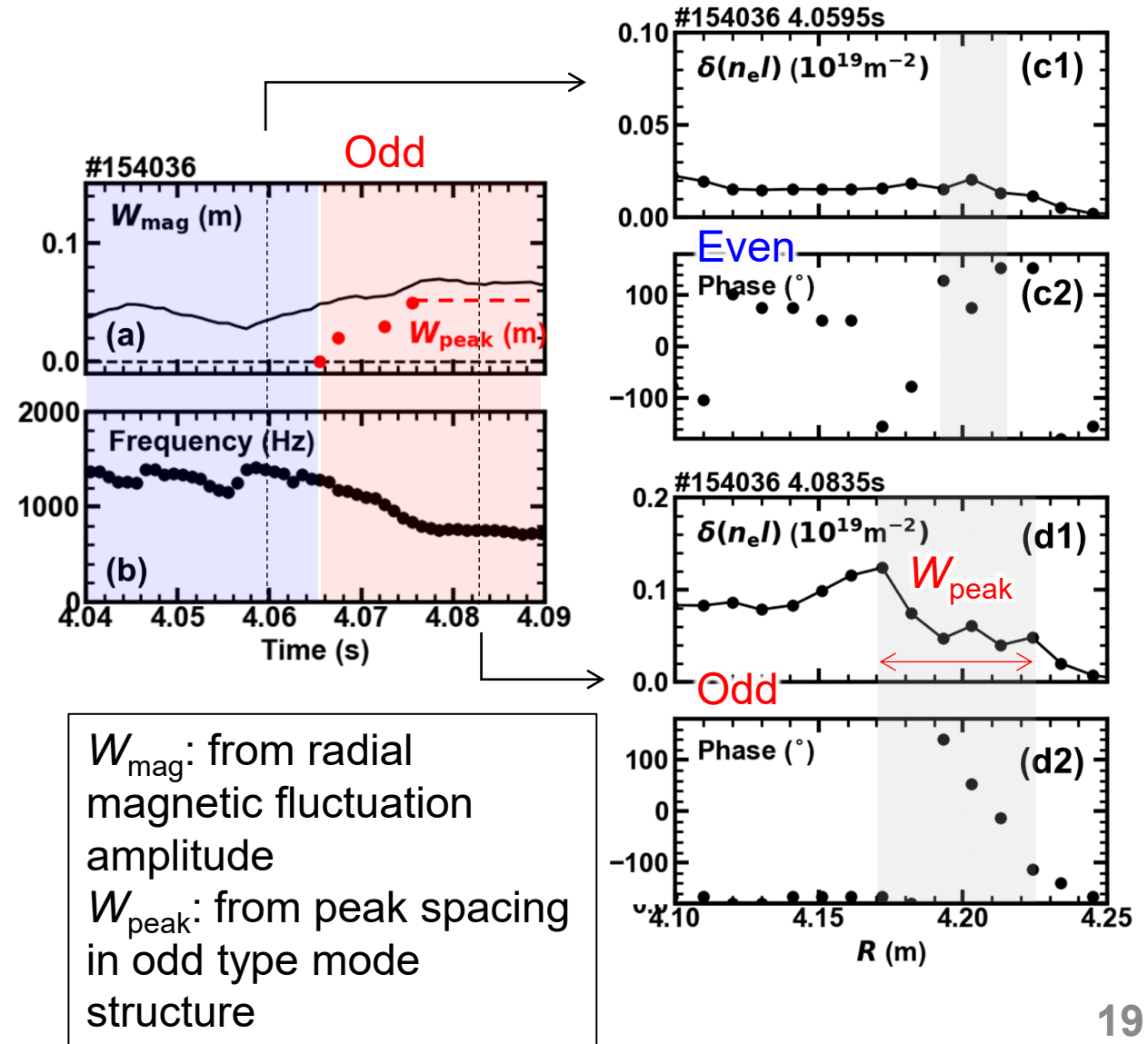
- From an even-parity mode to an odd-parity mode
- Or the reverse: from odd to even parity

→ **The first observation reported in LHD**
[Takemura et al., Scientific Reports, 2025]



Process of even-to-odd parity transition

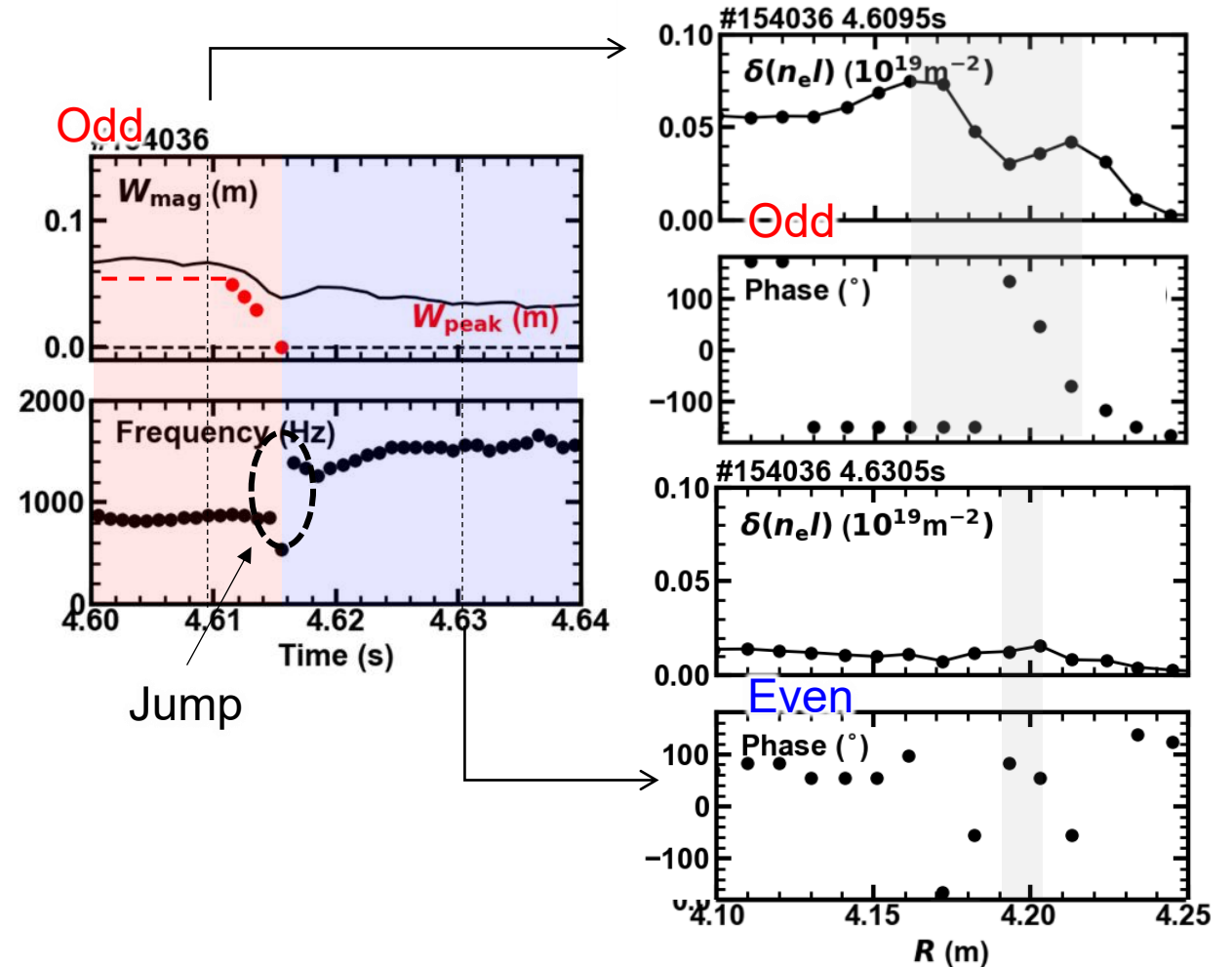
- At $t \sim 4.067$ s, W_{peak} is finite
→ **Island formation**
- Around $t \sim 4.06$ s, the magnetic fluctuation amplitude rapidly grows, and after 5 to 6 cycles, W_{peak} begins to expand
- W_{peak} saturates approximately 10 ms after the start of the expansion
 - W_{mag} and W_{peak} are in good agreement



Process of odd-to-even parity transition

- The timescale for the magnetic island to disappear is approximately 4 ms
- W_{peak} begins to decrease together with the reduction in mode amplitude
- The mode frequency abruptly increases after island disappearance

→ The observed parity transition is thought to result from the competition between even- and odd-parity modes.



Frequency determination mechanisms of MHD activities

Importance of Studying Frequency Characteristics of MHD Instabilities

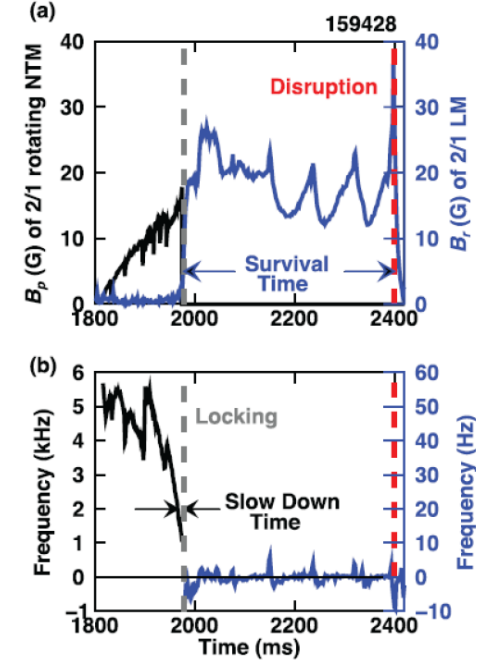
- Low-n MHD instabilities can lead to a rapid degradation of plasma confinement following a decrease in magnetic fluctuation frequency caused by the instability.

- **Locked mode in tokamaks** (Sweeney et al., 2017)
- **Locked-mode-like instability in LHD** (Sakakibara et al., 2015)

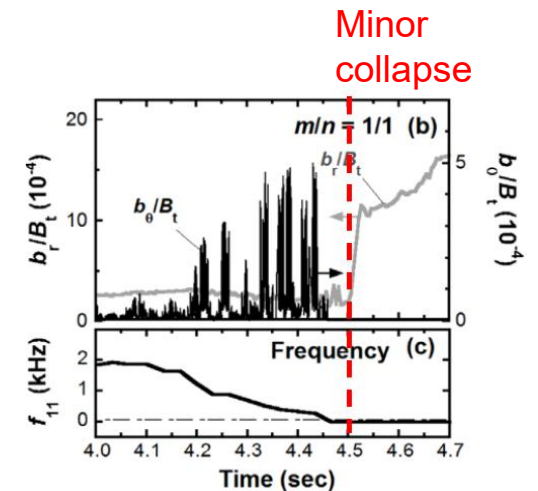
→ This study aims to clarify the physical mechanisms that determine the magnetic fluctuation frequency associated with MHD stability.

→ We investigate the frequency characteristics of MHD instabilities and compare them with existing torque balance models.

Locked mode (DIII-D)
[Sweeney2017]



LM-like inst. (LHD)
[Sakakibara2015]



Comparison between Observed δb - f Trajectories and the Torque Balance Model in LHD

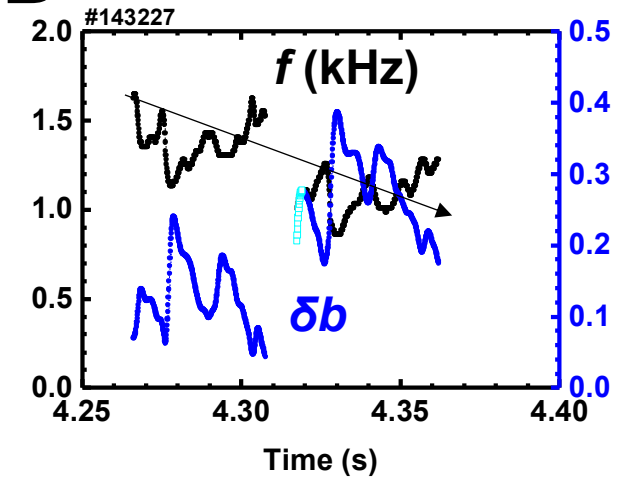
- In high-current LHD plasmas \rightarrow **Locked-mode-like instability** (Takemura et al., 2019; 2021)
 - The instantaneous frequency exhibits transient increases and decreases.
 - Despite these variations, **the δb - f trajectory follows the same path** during both frequency rise and fall.
- **This trajectory is consistent with the torque balance model** proposed by Fitzpatrick (1993), which includes:
 - **Driving force from viscous torque**
 - **Braking force due to $\mathbf{J} \times \mathbf{B}$ interaction with external RMPs**

Driving force NC viscosity $F_{VC} \equiv \mu(\omega_0 - \omega)$

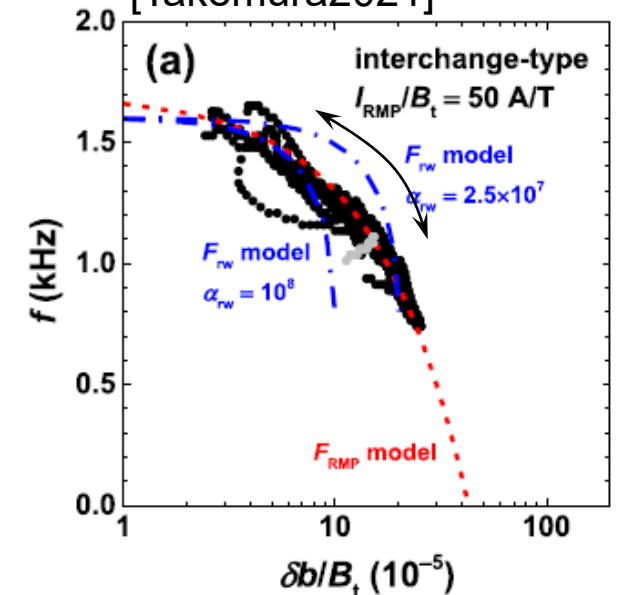
Braking force

$\mathbf{J} \times \mathbf{B}$ force between perturbed current due to instability and perturbed mag. field due to external RMP

$$F_{RMP} \equiv \delta b \delta b_{RMP} \frac{\omega \tau_v}{\sqrt{1 + \omega^2 \tau_v^2}} \quad \tau_v: \text{wall constant time}$$



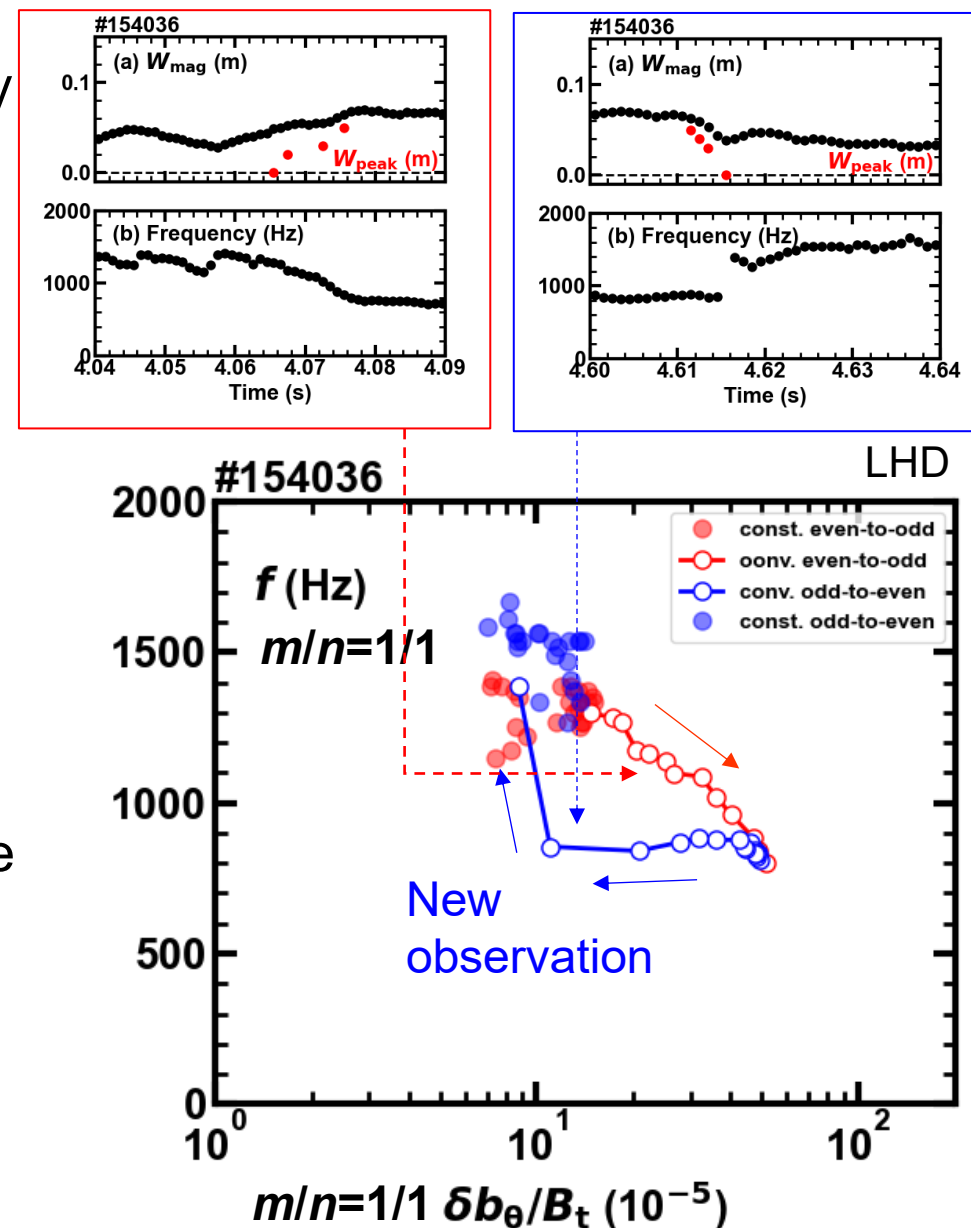
LM-like inst. (LHD)
[Takemura2021]



Observed Hysteresis in δb - f Trajectories

- In relatively high-density LHD plasmas, MHD instability with an island repeatedly grows and stabilizes (Takemura et al., 2021).
- A **hysteresis** is found in the δb - f trajectory
- **During the frequency-decreasing phase:**
 - The frequency gradually decreases in response to the increasing fluctuation amplitude.
- **During the frequency-increasing phase (a newly observed behavior):**
 - The frequency remains nearly constant even as the amplitude decreases, followed by a **sudden jump in frequency**.

→ This behavior **cannot be explained by conventional torque balance models**.



Interpretation of Hysteresis in the δb - f Trajectory

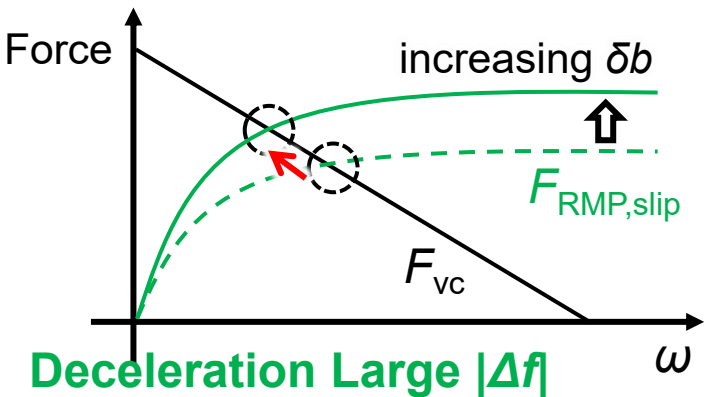
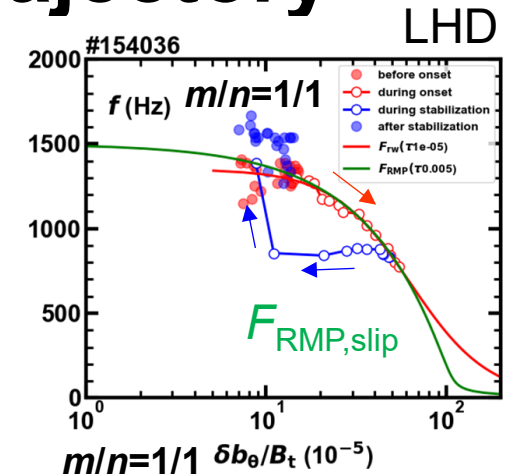
- The δb - f trajectory during the **frequency-decreasing phase** is consistent with the conventional F_{RMP} model.
- The unexplained nature of the frequency-increasing phase suggests that a new model is required for its interpretation.

- F_{RMP} no-slip model:

- A small frequency difference with the external RMP leads to strong RMP shielding.

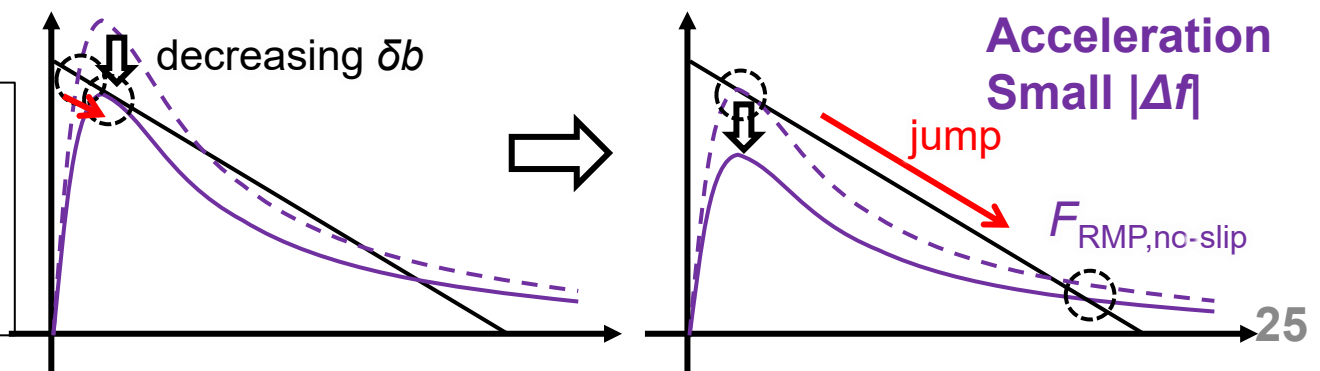
→ The frequency jump observed during the frequency-increasing phase can be qualitatively explained by the F_{RMP} no-slip model.

[FEC2025]



$$F_{\text{RMP,slip}} \equiv \delta b \delta b_{\text{RMP}} \frac{\omega \tau_v}{\sqrt{1 + \omega^2 \tau_v^2}} \quad (\text{large } |\Delta f|)$$

$$F_{\text{RMP,no-slip}} \equiv \delta b \delta b_{\text{RMP}} \frac{\omega \tau_v}{1 + \omega^2 \tau_v^2} \quad (\text{small } |\Delta f|)$$



Short Summary

Torque balance model incorporating RMP penetration

- The δb – f relationship can be derived from the torque balance model (Fitzpatrick, 1993).
- External RMPs driven by eddy currents induced by MHD instabilities may co-rotate with the plasma,
→ resulting in a possible “no-slip” state.

Braking $J \times B$	$F_{\text{RMP,slip}}$	$F_{\text{RMP,no-slip}}$	F_{rw}
Perturbed B	Ext. RMP with large Δf	Ext. RMP with small Δf	Eddy current
Perturbed j	Instability	Instability	Instability

Driving force (NC viscosity) $F_{\text{VC}} \equiv \mu(\omega_0 - \omega)$

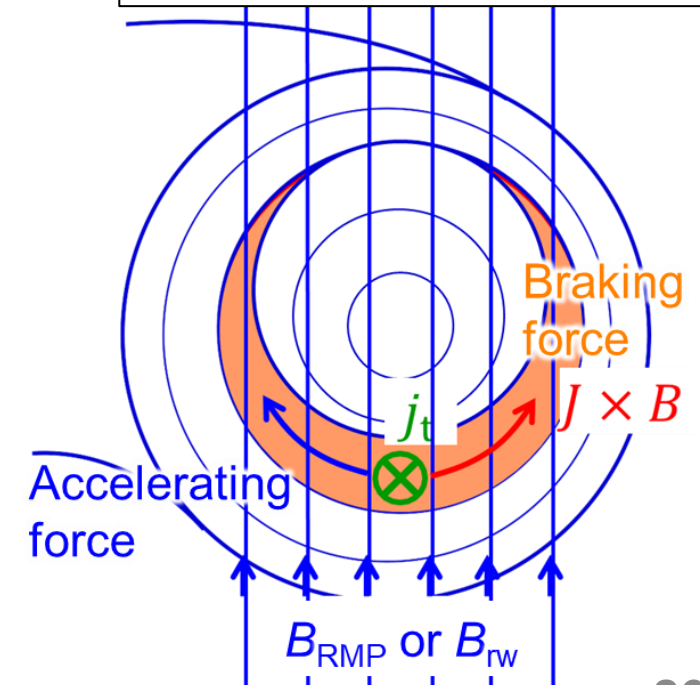
Braking force

$$F_{\text{RMP,slip}} \equiv \delta b \delta b_{\text{RMP}} \frac{\omega \tau_v}{\sqrt{1 + \omega^2 \tau_v^2}} \quad (\text{large } |\Delta f|)$$

$$F_{\text{RMP,no-slip}} \equiv \delta b \delta b_{\text{RMP}} \frac{\omega \tau_v}{1 + \omega^2 \tau_v^2} \quad (\text{small } |\Delta f|)$$

$$F_{\text{rw}} \equiv \delta b^2 \frac{\omega \tau_v}{1 + \omega^2 \tau_v^2} \quad (\text{small } |\Delta f|)$$

τ_v : a function of T , n , and shape factor
 δb_{RMP} : external RMP amplitude
 ω_0 : rotation frequency determined by viscosity, and it depends on n , T , shape factor, and gradient



AI-Assisted Prediction of Abrupt MHD Events

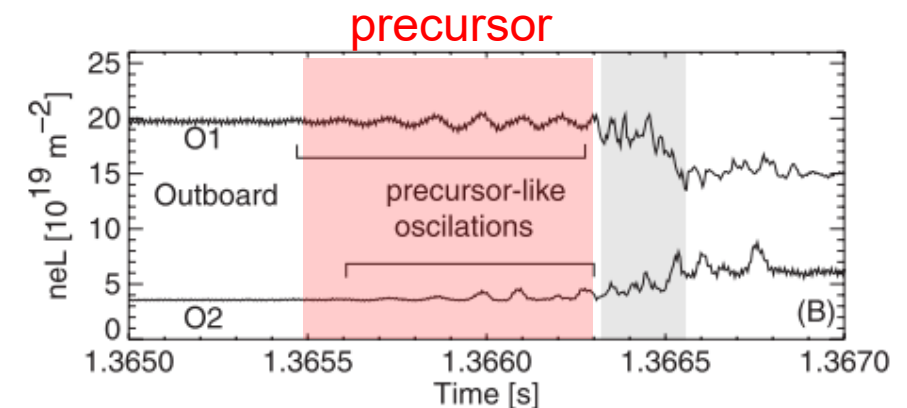
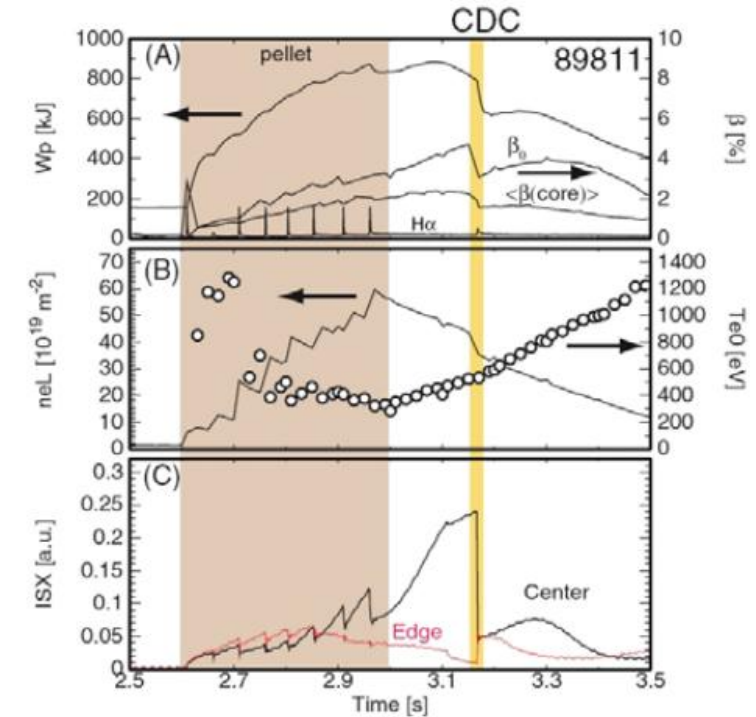
Abrupt event with International Collaboration

- Understanding and predicting **abrupt plasma phenomena** is critically important for advancing fusion research.
 - In LHD, various abrupt events such as the Energetic-ion-driven Interchange Mode (EIC) and **Core Density Collapse (CDC)** have been observed.
[EIC: Du et al., PRL, 2015], [CDC: Ohdachi et al., Nuclear Fusion, 2017]
 - To better understand the fast dynamics of CDC, **international collaborative research is underway**:
 - Rotational transform profile measurements during CDC are being conducted in collaboration **with IPP, Germany**
 - Pressure profile evolution during CDC is being investigated using a high-repetition Thomson scattering system (**fast TS**) **with University of Wisconsin–Madison**
- ✂A formal collaboration agreement has been signed with the UW-M
- Due to the short measurement time of fast TS, advance event prediction and timely triggering are required

Abrupt event in LHD—Core Density Collapse—

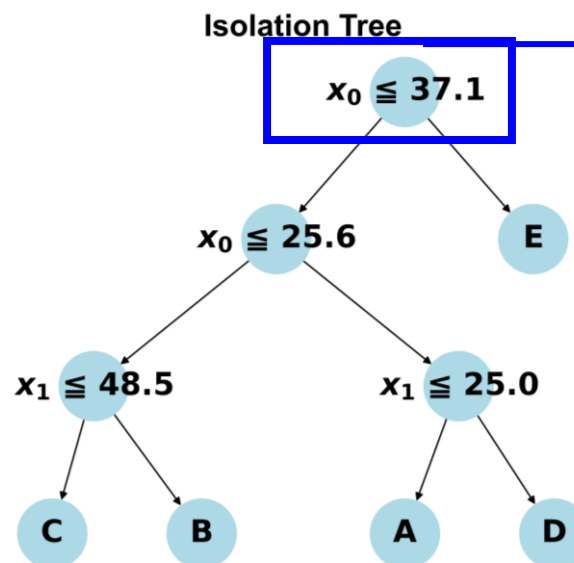
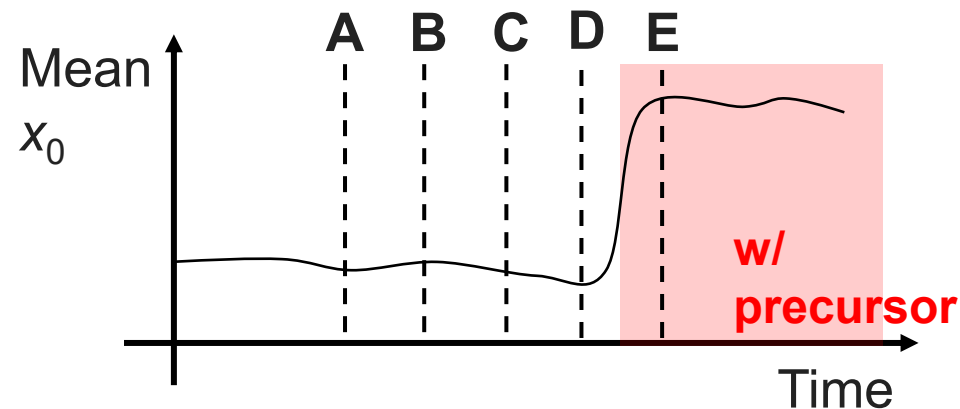
- Injection of multiple pellets into LHD plasmas enables the formation of super central density plasmas
 - One of the operational scenarios aimed at achieving high-performance plasma conditions
- In such plasmas, core density collapse (CDC) events have been observed [S. Ohdachi et al., Nucl. Fusion, 2017]
 - The collapse proceeds very rapidly, typically within a few milliseconds
- Just before the collapse, precursor oscillations in the density signal are often observed
- However, due to variations in waveform patterns, simple threshold-based detection is difficult

→ A machine learning-based method has been developed for detecting precursor oscillations

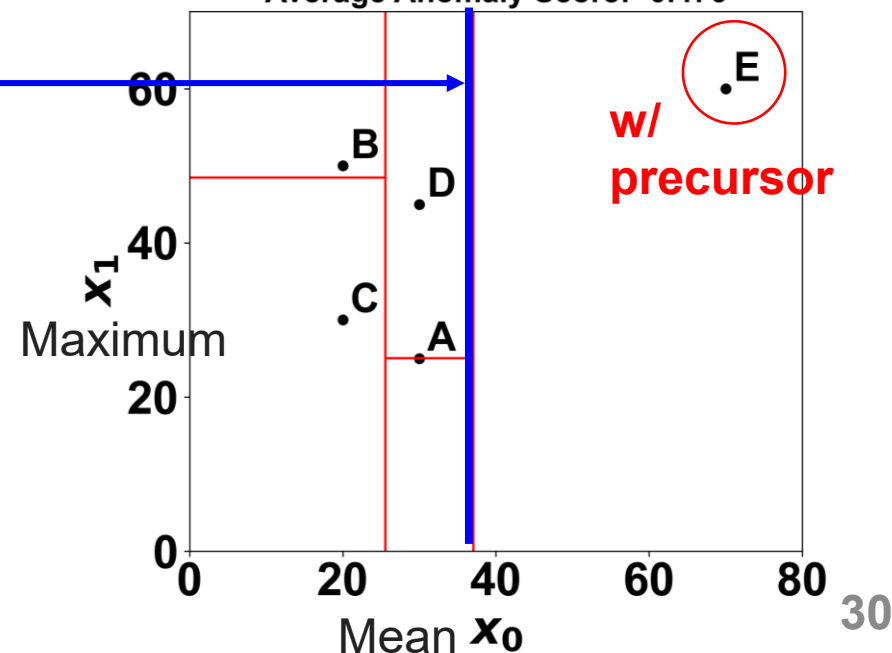


Anomaly detection using Isolation Forest

- For unsupervised, fast, and lightweight anomaly detection, the Isolation Forest is employed
 - Data are split based on randomly selected features and thresholds to construct decision trees
 - Anomalies are more easily isolated
 - A shorter path to the leaf (i.e., a lower anomaly score) indicates anomaly
 - The data are classified as anomalous or normal based on a threshold comparison
- Anomaly score $-2^{\frac{E}{c}}$
- The average path length E across all isolation trees

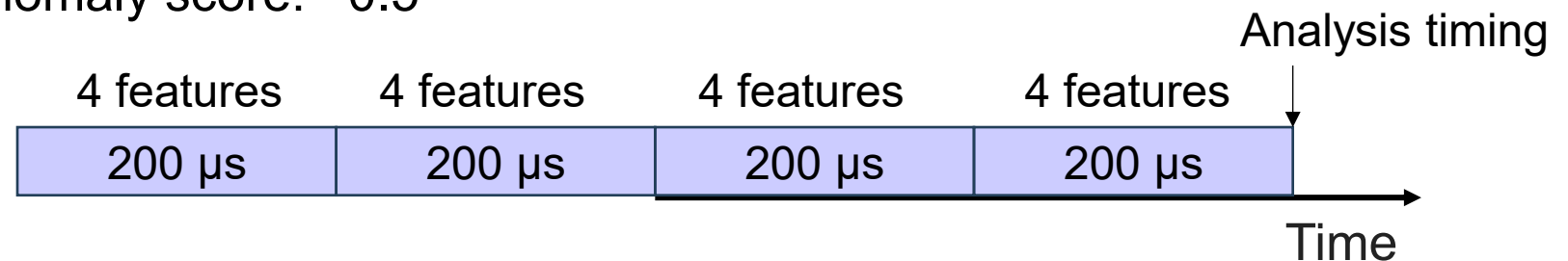


2D Partitioning from Isolation Tree
(n_estimators=1, max_samples=5, random_state=11)
Average Anomaly Score: -0.476



Parameter Settings for Isolation Forest

- Use electron density signals at 1 MS/s
- 16 features in total
 - Four basic features are considered: mean, maximum, minimum, and peak-to-peak value
 - A window of 800 μs is divided into four segments, and features are calculated for each segment
 - Selected features, window length and the number of segments are optimized
- Number of weak learners (decision trees): 100
 - Too many trees may lead to overfitting and high computational cost, while too few may reduce accuracy.
- Number of samples per tree (sub-dataset size): 1024
- Threshold for the anomaly score: -0.5



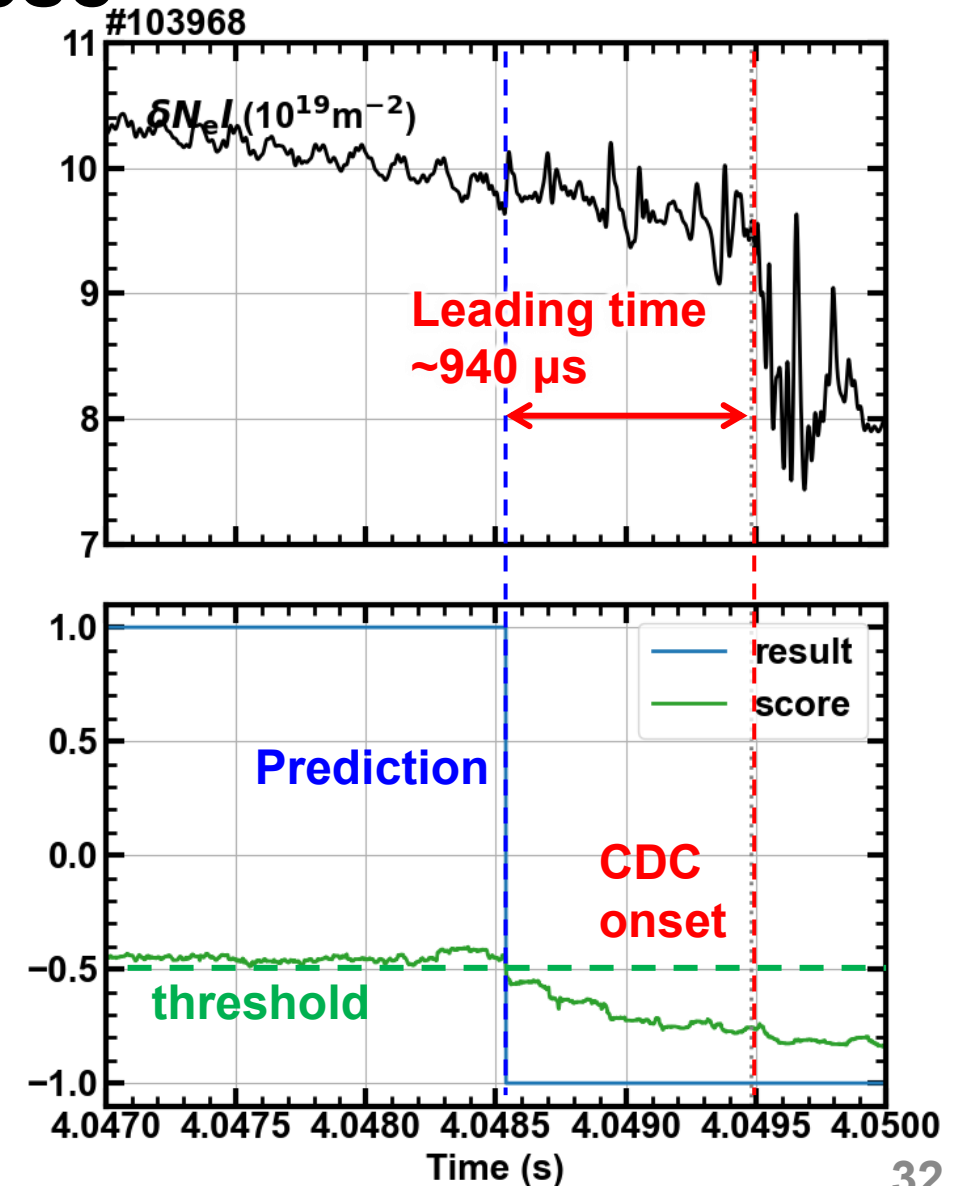
Successful prediction several hundred microseconds before the collapse

- Leave-One-Out Cross Validation (LOOCV) was performed using 10 CDC discharges
 - nine for training and one for testing
- CDC onsets were successfully predicted on average about 300 μs , with the earliest prediction occurring up to 960 μs in advance

→ The leading time is within the $\sim 200 \mu\text{s}$ delay of fast TS in LHD

CDC onset:

The time derivative of the electron density exceeded the threshold within 1 ms.

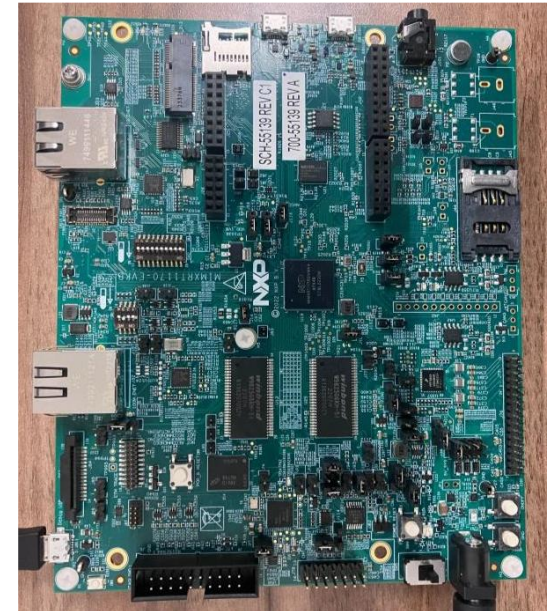


Real-time trigger device with microcontroller implementation

- The algorithm was implemented on a microcontroller to develop a trigger-generation device
- The microcontroller platform, [MIMXRT1170-EVKB](#)
 - a high-speed clock (up to 1 GHz), large memory resources, and support for real-time processing
 - Accepts analog input and provides digital output (TTL) signals to issue diagnostic triggers.
- Analog signals are digitized at 1 MHz using the microcontroller's built-in A/D converter
- [Anomaly scores are computed every 10 \$\mu\$ s](#)
- The model is trained offline in Python using Isolation Forest. In real time, anomaly scores are computed in C by comparing extracted features with a preset threshold

→ Planned for LHD validation in late 2025, the system targets real-time prediction and diagnostic triggering

MIMXRT1170-EVKB
manufactured by NXP
Semiconductors



Summary

- This presentation highlights recent MHD research in LHD to encourage collaborative studies within the helical device community.
- 1. **Stabilization of resistive interchange modes by external RMPs**
- 2. **Island dynamics based on Parity transitions in MHD mode structure**
- 3. **Frequency dynamics and δb -f hysteresis analysis**
- 4. **AI-assisted prediction of abrupt events (e.g., CDC)**
- **LHD experimental proposals are open from June 2–13, 2025**
 - The experiments will be conducted from mid-September to the end of December 2025